Title

Regioselective Termination Reagents for Ring-Opening Alkyne Metathesis Polymerization

Journal

Journal of the American Chemical Society, 139(43)

ISSN

0002-7863

Authors

Jeong, Hyangsoo

von Kugelgen, Stephen

Bellone, Donatela

et al.

Publication Date

2017-11-01

DOI

10.1021/jacs.7b09390

Peer reviewed

Regioselective Termination Reagents for Ring-Opening Alkyne Metathesis Polymerization

Hyangsoo Jeong,[†] Stephen von Kugelgen,[†] Donatela Bellone,[†] and Felix R. Fischer[†‡§*]

[†]Department of Chemistry, University of California Berkeley, Berkeley, CA 94720, United States

[‡]Materials Science Division, Lawrence Berkeley National Laboratory, Berkeley, CA 94720, United States

[§]Kavli Energy NanoSciences Institute at the University of California Berkeley and the Lawrence Berkeley National Laboratory, Berkeley, CA, 94720, United States

ABSTRACT: Alkyne cross-metathesis of molybdenum carbyne complex [TolC≡Mo(OCCH$_3$(CF$_3$)$_2$)$_3$]•DME with two equivalents of functional ynamines or ynamides yield the primary cross-metathesis product with high regioselectivity (> 98%) along with a molybdenum metallacyclobutadiene complex. NMR and X-ray crystal structure analysis reveals that ynamides derived from 1-(phenylethynyl)pyrrolidin-2-one selectively cleave the propagating molybdenum species in the ring-opening alkyne metathesis polymerization (ROAMP) of ring-strained 3,8-dihexyloxy-5,6-dihydro-11,12-didehydrodibenzo[*a*,*e*][8]annulene and irreversibly deactivate the diamagnetic molybdenum metallacyclobutadiene complex through a multidentate chelate binding mode. The chain-termination of living ROAMP with substituted ethynylpyrrolidin-2-ones selectively transfers a functional end-group to the polymer chain giving access to telechelic polymers. This regioselective carbyne-transfer strategy gives access to amphiphilic block-copolymers through synthetic cascades of ROAMP followed by ring-opening polymerization (ROP) of strained ε-caprolactone.

INTRODUCTION

Living ring-opening olefin metathesis polymerization (ROMP) initiated by well-defined and functional-group-tolerant catalysts has been a powerful polymerization technique since its initial discovery in the 1960s.[1] The unique ability to transfer a functional group to the end of a growing polymer chain by using either a chain-transfer or -termination agent made ROMP a particularly interesting method to access functional telechelic polymers.[2,3] The propagating species in ROMP with highly oxophilic molybdenum carbene complexes can be irreversibly terminated by reaction with substituted benzaldehydes to generate polymers featuring a functional styryl end-group and an inactive molybdenum oxo complex.[4–6] Ruthenium-based ROMP catalysts instead react with substituted vinyl ethers to form deactivated Fischer-type carbene complexes leaving behind a polymer chain with desired functional group.[7–9] Selective incorporation of functional end-groups has expanded the application of ROMP toward biologically active polymers,[10] biomimetic block copolymers,[11] self-assembled brush copolymers,[12–14] and polymer surface functionalization.[15,16] An irreversible termination reaction for the analogous ring-opening alkyne metathesis polymerization (ROAMP), capable of installing a variety of functional end-groups on a growing polymer chain has not been reported in the literature. Here we describe a highly regioselective, irreversible carbyne-transfer reaction between a substituted ynamide and a living polymer chain initiated by molybdenum benzylidyne ROAMP catalyst. The reaction not only introduces a functional end-group into the polymer chain but irreversibly traps the ROAMP initiator as a catalytically inactive molybdenum metallacyclobutadiene complex. This protocol provides access to well-defined block-copolymers via orthogonal ring-opening polymerizations.

RESULTS AND DISCUSSION

Inspired by the reaction of tetraalkyldiaminoethylenes with molybdenum benzylidyne complexes reported by Tamm, who showed that the intermediate dialkylamino molybdenum carbyne reacts regioselectively with ynamines to form stable metallacyclobutadiene complexes,[17] we explored the cross-metathesis of [TolC≡Mo(OCCH$_3$(CF$_3$)$_2$)$_3$]•DME (**1**), a model complex for the propagating polymer chain in the ROAMP mechanism, with ynamine **2a** and ynamides **2b**-**e** (Scheme 1).

Scheme 1. Irreversible Regioselective Termination of a Molybdenum Carbyne Complex with Ynamines and Ynamides.

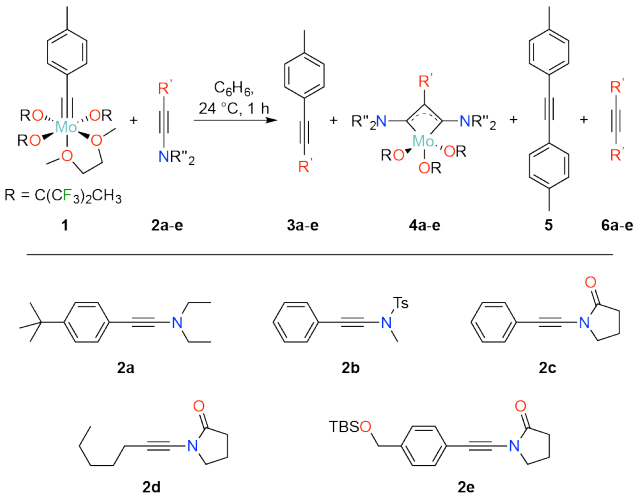

Reaction of molybdenum complex **1** with 2 equiv of **2a** yields a mixture of asymmetrically substituted tolane **3a** and a paramagentic metallacyclobutadiene complex **4a**. The unusual regioselectivity inherent to our termination reaction relies on the electron-donating N-atom in **2a** that induces a partial polarization of the triple bond.[18] The initial cross-metathesis preferably places the electron-rich end of the C≡C bond in **2a** next to the electron deficient Mo center in **1**, thus favoring the transfer of the end-group (R' in Scheme 1) to the tolane **3a**.[19] A second equiv of **2a** reacts with the intermediate Mo carbyne complex to give the metallacyclobutadiene complex **4a**. Besides the expected products **3a** and **4a** GCMS reveals a series of symmetric tolanes **5** and **6a** (<7 %) in the crude reaction mixture that result from uncontrolled cross-metathesis reactions (Figure S1). As the generation of the undesired symmetric side products could not be inhibited by addition of excess **2a** we sought to stabilize the deactivated metallacyclobutadiene complex **4a** by introducing secondary metal binding sites that favor chelation of the Mo center.

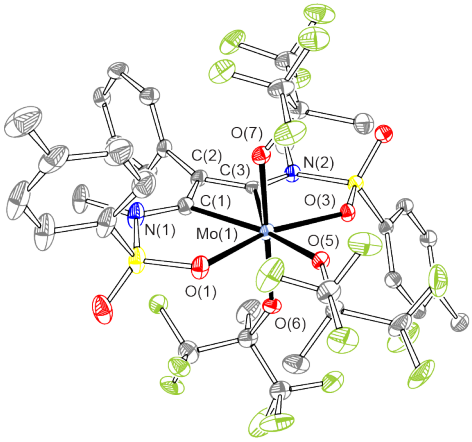

Figure 1. Single-crystal X-ray structures of **4b**. Thermal ellipsoids are drawn at the 40% probability level. Color coding: C (gray), O (red), F (green), Mo (turquoise), N (blue), S (yellow). Hydrogen atoms are omitted for clarity.

Table 1. Product distribution of the organic fraction resulting from the reaction of 1 with 2a-c determined by GCMS.

reagent	3a-c	5	6a-c
2a	93%	1%	6%
2b	99%	<0.5%	<0.5%
2c	99%	<0.5%	<0.5%

We investigated the cross-metathesis of **1** with 2 equiv of the terminating reagent **2b** featuring a toluene sulfonamide group. ^{19}F NMR reveals a complete consumption of **1** within 20 min at 24 °C. ^{1}H NMR shows the formation of 1-methyl-4-(phenylethynyl)benzene (**3b**) as the only cross-metathesis product, next to a series of paramagnetically shifted resonances that were assigned to the metallacyclobutadiene complex **4b**. Orange prisms of **4b** suitable for X-ray crystallography were obtained from saturated toluene/Et_2O (1:1) solutions at –25 °C. In the crystal **4b** adopts a pentagonal bipyramidal geometry around the Mo center (Figure 1). The metallacyclobutadiene ring rests in the equatorial plane and bears two N,4-dimethylbenzenesulfonamide substituents at the α-carbons and a phenyl ring at the β-position. Both sulfone groups coordinate *trans* to the Mo center through one of their oxygen atoms, hindering subsequent metatheses. Two hexafluoro-*tert*-butoxide ligands occupy the axial positions of the complex while a third alkoxide ligand is coordinated *trans* to the metallacyclobutadiene ring. The Mo(1)–C(1) and Mo(1)–C(3) distances are 2.166(3) Å and 2.154(3) Å respectively, closer to the expected length of a Mo–C single bond (~2.14 Å) than a Mo=C double bond (~1.87 Å).[20] The C(1)–C(2) (1.388(5) Å) and C(2)–C(3) (1.395(5) Å) bonds forming the backbone of the four membered ring adopt intermediate lengths between a $C(sp^2)$–$C(sp^2)$ single and a $C(sp^2)$=$C(sp^2)$ double bond.[21] Short C(1)–N(1) and C(3)–N(2) bonds, 1.332(5) Å and 1.330(5) Å respectively, suggest an extended delocalization along the N(1)–C(1)–C(2)–C(3)–N(2) ligand backbone. This structure is in marked contrast to the high-oxidation-state tungsten metallacyclobutadiene solid-state structure reported in the literature featuring clear single- and double-bond alternation in the metallacyclobutadiene ring.[22–27] Magnetic susceptibility measurements using the Evans' method reveal that the ground state of **4b** is a triplet (μ_{eff} = 2.75 μ_B in toluene). Density functional theory (DFT) calculations show that the triplet (S = 1) state of **4b** is stabilized by ΔG_{298} = 12.56 kcal mol^{-1} with respect to the singlet (S = 0). Mulliken population analysis suggests that 80% of the two SOMOs are localized on the Mo center further supporting the formation of **4b** as a high-spin d^2 Mo(IV) species (Supporting Information, Figure S3). The electronic structure **4b** is reminiscent of high-spin d^2 Mo(IV) metallacyclobutadiene complexes generated from the reaction of [MesC≡Mo(OCCH$_3$(CF$_3$)$_2$)$_3$] (Mes = 2,4,6-trimethylphenyl) with diaminoacetylenes recently reported by Tamm.[17]

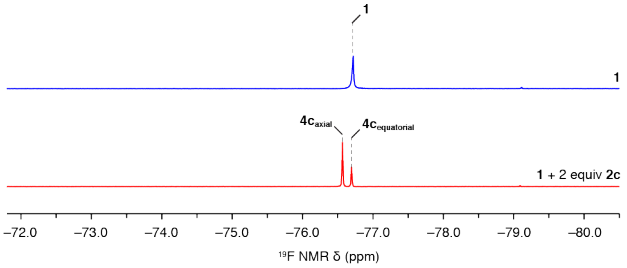

Figure 2. ^{19}F NMR spectroscopy of crude reaction mixtures following the reaction of **1** with 2 equiv **2c** (564 MHz, 24 °C in C_6D_6, sealed NMR tube).

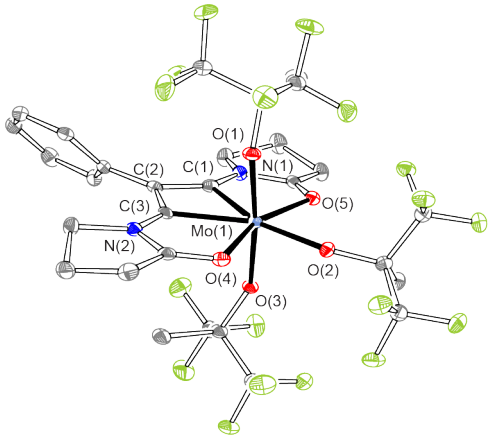

Figure 3. Single-crystal X-ray structures of **4c**. Thermal ellipsoids are drawn at the 40% probability level. Color coding: C (gray), O (red), F (green), Mo (turquoise), N (blue). Hydrogen atoms are omitted for clarity.

While the reaction of **1** with 2 equiv of **2b** proceeds to full conversion and could effectively terminate the propagating chain in a ROAMP reaction, the difficulty of monitoring the formation of paramagnetic **4b** along with the limited stability of **4b** in solution represents significant shortcomings. Expanding on this initial success we explored the use of 2-pyrrolidone groups as chelating substituents on the terminating reagent. 2-pyrrolidone not only has been shown to slow the metathesis activity of Schrock's molybdenum alkylidene complexes,[28] but readily adopts a geometry reminiscent of the chelating binding mode of sulfonamides in **4b** required to further stabilize the deactivated molybdenum metallacyclobutadiene complex. Cross-metathesis of **1** with 2 equiv of 1-(phenylethynyl)pyrrolidin-2-one (**2c**) yields an orange solid in 83% yield after fractional recrystallization. ^{1}H NMR and GCMS (Figure S2) of the crude reactions mixture show the formation of only the desired asymmetric cross-metathesis product **3c** (>98%). To our surprise the sharp resonances in ^{1}H and ^{19}F NMR attributed to the metallacyclobutadiene complex indicate that **4c** has a diamagnetic ground state. Orange plates of **4c** suitable for X-ray crystallography were obtained from saturated Et_2O solutions at –25 °C. In the solid state the coordination geometry of **4c** is isostructural to **4b** (Figure 3). The Mo(1)–C(1) and Mo(1)–C(3) distances in **4c** are shorter, 2.108(3) Å and 2.109(3) Å respectively, while the C(1)–N(1) and C(3)–N(2) distances 1.366(4) Å and 1.364(4) Å increase by about the same amount. We attribute these subtle changes in bond lengths around the metallacyclobutadiene to a more efficient delocalization of the nitrogen lone pair towards the amide carbonyl that leads to a diminished contribution to the conjugation in the N(1)–C(1)–C(2)–C(3)–N(2) ligand backbone. The pentagonal bipyramidal geometry is retained in solution. ^{19}F NMR spectra of **4c** show two sharp singlets at –76.7 ppm and –76.8 ppm (2:1) assigned to the axial and equatorial alkoxides (Figure 2). DFT calculations confirm that the diamagnetic (S = 0) ground state of **4c** is stabilized by ΔG_{298} = 5.24 kcal mol^{-1} with respect to the lowest triplet state (S = 1). Moreover, the diamagnetic complex **4c** is stable in solution at 24 °C.

Scheme 2. Regioselective Termination of ROAMP of 7 with 2a-e.

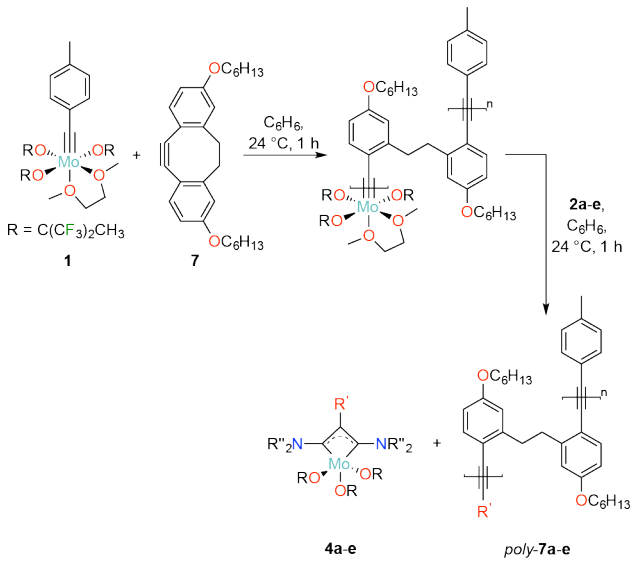

Table 2. Molecular weight analysis of *poly*-7a-e.

reagent	M_n theory	M_n (SEC)[a]	M_w (SEC)[a]	X_n	$Đ_M$ (M_w/M_n)
2a	4290	8100	11800	16	1.5
2b	4240	5200	8000	12	1.5
2c	4240	6200	9100	13	1.5
2d	4230	8900	11300	24	1.5
2e	4380	6000	8400	13	1.4

[a] Size exclusion chromatography (SEC) calibrated to polystyrene standards. [b] degree of polymerization determined by ^{1}H NMR end-group analysis.

Scheme 3. Synthesis of ROAMP-ROP block copolymer *poly*-7e-*block*-εCL from telechelic macroinitiator *poly*-7e

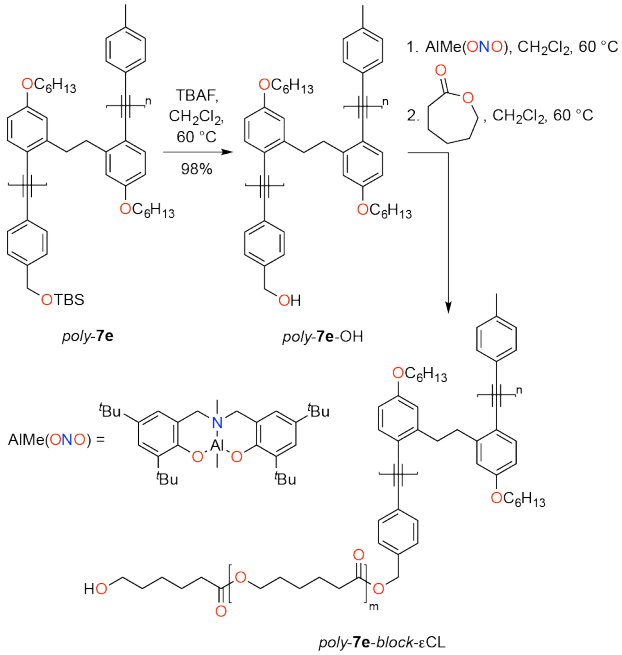

Taking advantage of the irreversible cross-metathesis with **2c** described above we studied the termination of ROAMP of 3,8-dihexyloxy-5,6-dihydro-11,12-didehydrodibenzo[*a*,*e*][8]annulene (**7**) with **1** (Scheme 2). Upon addition of **7** to a solution of **1** in benzene ([**7**]/[**1**] = 10) at 24 °C the ring-strained monomer is consumed in less than 1 h. Termination of the living polymer chains with two equiv of **2c** leads to an instantaneous color change of the reaction mixture from yellow to orange. By ^{1}H and ^{19}F NMR we observe the formation of metallacyclobutadiene **4c**. Precipitation of the terminated polymers in MeOH/hexane yields *poly*-**7c** in greater than 80% isolated yield. Size-exclusion chromatography (SEC) analysis of isolated polymers shows a $Đ_M$ of 1.5. The molecular weights of *poly*-**7c** determined by SEC, calibrated to polystyrene standards are proportional to the initial [**7**]/[**1**] loading, and show a unimodal distribution. Addition of terminating agent does not lead to a broadening of the $Đ_M$. Table 1 summarizes the SEC analysis (M_n, M_w, and $Đ_M$) for ROAMP polymers terminated with **2a-e**. As a control experiment, excess 3-hexyne (13 equiv) was tested as a terminating agent. The resulting polymers contained a mixture of end-groups resulting from solvolysis of unterminated catalysts (CH_3 and CH_2OH) and butynyl end-groups from 3-hexyne by MALDI-TOF (Figure S5).[29]

MALDI-TOF mass spectra of isolated *poly*-**7a-c** show discrete families of signals that correspond to the mass of polymers featuring the unique end-group R' transferred from **2a-c** during the termination step (Figure 4A, Supporting Information, Figure S6–S15). In an effort to evaluate the steric demand of a terminating agent on the rate of cross-metathesis we reacted alkyl substituted pyrrolidinone **2d** with living ROAMP polymer chains. Following an initial transfer, the heptyne end-group is sterically less hindered than the internal triple bonds in the polymer chain and readily undergoes chain-transfer extension with residual unterminated living polymer chains. This observation is consistent with previous reports[29] and is reflected in the unusually high degree of polymerization (X_n = 24) of *poly*-**7d** determined by ^{1}H NMR end-group analysis.

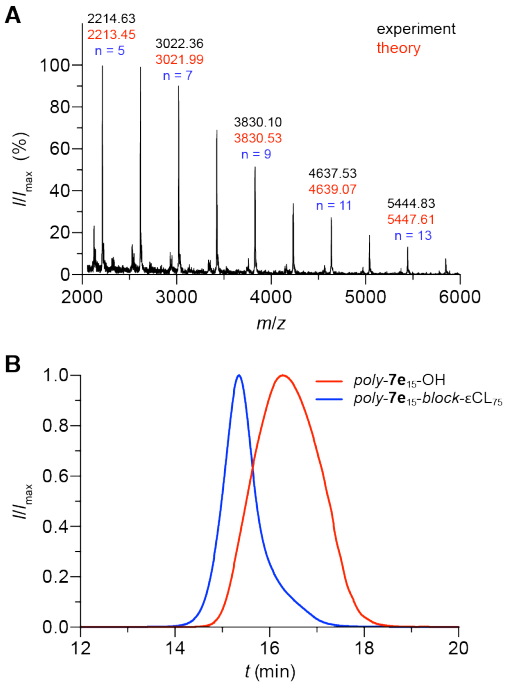

Figure 4. A) MALDI-TOF mass spectra of isolated *poly*-**7c**. B) SEC traces showing the chain extension of macroinitiator *poly*-**7e** (red) to give *poly*-**7e**$_{15}$-*block*-εCL_{75} (blue); calibrated to polystyrene standards.

Functionalized terminating reagents derived from **2c** not only provide a practical tool to control polymer chain length by irreversibly cleaving and deactivating the propagating Mo ROAMP catalyst, but the unique regioselectivity of the cross-metathesis with ynamides provides access to telechelic polymers. Termination of a propagating chain with **2e**, a (phenylethynyl)pyrrolidinone featuring a *tert*-butyldimethylsilyl (TBS) protected benzyl alcohol, provides access to competent macroinitiators for lactone ring-opening polymerization. Unlike **2a-d**, ROAMP termination with **2e** does not go to completion (~80% by ^{1}H NMR analysis). Along unterminated *poly*-**7** the crude reaction mixture contains traces of a polymer species featuring a pyrrolidone end-group, which could be observed by MALDI-TOF but remains below the detection limit of ^{1}H NMR spectroscopy. Deprotection of the TBS group in *poly*-**7e** with tetrabutylammonium fluoride (TBAF) yields polymers featuring a benzyl alcohol end-group (*poly*-**7e**-OH) in > 98% yield (Scheme 3). The progress of the reaction can readily be monitored by ^{1}H NMR spectroscopy or MALDI-TOF mass spectrometry (Supporting Information, Figure S16–S17). Treatment of this macroinitiator *poly*-**7e**-OH with a lactone ring-opening polymerization (ROP) catalyst AlMe(ONO) [ONO = (CH_3)N-$(CH_2$-2-O-3,5-$C_6H_2(t$Bu$)_2)_2$] followed by addition of 100 equiv of ε-caprolactone (εCL) gives crude *poly*-**7e**-*block*-εCL in > 74% yield (Figure S18).[30] The amphiphilic block copolymer can be isolated from a small amount of residual unfunctionalized *poly*-**7** (<5% by ^{1}H NMR analysis) or from trace polymers containing pyrrolidone end-groups (only detected in MALDI-TOF mass spectrometry) by fractional precipitation from THF. SEC shows an apparent increase in molecular weight from 6.5 kDa in *poly*-**7e**-OH to 16.5 kDa in *poly*-**7e**-*block*-εCL corresponding to *poly*-**7e**$_{15}$-*block*-εCL_{75} by ^{1}H NMR end-group analysis (Figure 4). The living ROP chain-extension of telechelic *poly*-**7e**-OH macromonomers with εCL not only introduces a polar polymer building block but leads to an overall narrowing of the molecular weight distribution ($Đ_M$ = 1.2).

CONCLUSION

We herein report the highly regioselective cross-metathesis reaction of a molybdenum benzylidyne complex [TolC≡Mo$(OCCH_3(CF_3)_2)_3$]•DME with ynamine and ynamides. While reactions of ynamides derived from toluene sulfonamide generate paramagnetic metallacyclobutadiene species, reactions of ynamides featuring a 2-pyrrolidone group yield stable diamagnetic complexes. We demonstrated that ynamides are competent termination reagents that selectively and irreversibly react with the propagating species in the ROAMP of strained alkynes initiated by molybdenum benzylidyne catalysts. Functional aryl end-groups incorporated into ynamide termination reagents are selectively transferred to the propagating polymer chain end giving access to telechelic polymers. The versatility of this regioselective termination strategy is demonstrated by the synthesis of amphiphilic block-copolymers through a sequence of ROAMP and ROP of ε-caprolactone.

EXPERIMENTAL SECTION

Materials and General Methods. Unless otherwise stated, all manipulations of air and/or moisture sensitive compounds were carried out in oven-dried glassware, under an atmosphere of Ar or N_2. All solvents and reagents were purchased from Alfa Aesar, Spectrum Chemicals, Acros Organics, TCI America, and Sigma-Aldrich and were used as received unless otherwise noted. Organic solvents were dried by passing through a column of alumina and were degassed by vigorous bubbling of N_2 or Ar through the solvent for 20 min. Flash column chromatography was performed on SiliCycle silica gel (particle size 40–63 μm). Thin layer chromatography was carried out using SiliCycle silica gel 60 Å F-254 precoated plates (0.25 mm thick) and visualized by UV absorption. All ^{1}H, {^{1}H} ^{13}C, and ^{19}F NMR spectra were recorded on Bruker AV-300, AV-600, DRX-500, AV-700 and AV-500 spectrometers, and are referenced to residual solvent peaks ($CDCl_3$ ^{1}H NMR δ = 7.26 ppm, {^{1}H} ^{13}C NMR δ = 77.16 ppm; C_6D_6 ^{1}H NMR δ = 7.16 ppm, {^{1}H} ^{13}C NMR δ = 128.06 ppm; Toluene-d_8 ^{1}H NMR δ = 2.08 ppm) or hexafluorobenzene (^{19}F NMR δ = –162.90 ppm). High-resolution mass spectrometry (EI) was performed on a Autospec Premier (Waters) sector spectrometer in positive ionization mode. ESI mass spectrometry was performed on a Finnigan LTQFT (Thermo) spectrometer in positive ionization mode. MALDI mass spectrometry was performed on a Voyager-DE PRO (Applied Biosystems Voyager System 6322) in positive mode using a matrix of dithranol or dithranol/1% $AgNO_3$. Elemental analysis (CHN) was performed on a Perkin Elmer 2400 Series II combustion analyzer (values are given in %). Size-exclusion chromatography (SEC) was carried out on a LC/MS Agilent 1260 Infinity set up with a guard and two Agilent Polypore 300 x 7.5 mm columns at 35 °C. All SEC analyses were performed on a 0.2 mg/mL solution of polymer in chloroform. An injection volume of 25 μL and a flow rate of 1 mL/min were used. Calibration was based on narrow polydispersity polystyrene standards ranging

from M_w = 100 to 4,068,981. X-ray crystallography was performed on APEX II QUAZAR, using a Microfocus Sealed Source (Incoatec IμS; Mo-Kα radiation), Kappa Geometry with DX (Bruker-AXS build) goniostat, a Bruker APEX II detector, QUAZAR multilayer mirrors as the radiation monochromator, and Oxford Cryostream 700 for **4b** and **4c**. Crystallographic data was solved with SHELXT, refined with SHELXL-2014, visualized with ORTEP-32, and finalized with WinGX. Compounds **1**,[31] **7**,[31] **2b**,[32] **2c**,[33] and catalyst AlMe(ONO)[30] were synthesized following literature procedures.

Preparation of Metallacyclobutadiene (**4b**) A 25 mL vial was charged with [TolC≡Mo(OCMe(CF$_3$)$_2$)$_3$(DME)] (**1**) (50.9 mg, 0.061 mmol) in benzene (6 mL). A solution of *N*,4-dimethyl-*N*-(phenylethynyl)benzenesulfonamide (**2b**) (34.9 mg, 0.122 mmol) in benzene (2 mL) was added. After 1 h, the reaction mixture was concentrated in vacuum. The crude mixture was triturated with pentane and **4b** (33 mg, 48 %) was collected as a light brown solid. ^{1}H NMR (500 MHz, toluene-d_8, 0 °C) δ = 22.10 (6H), 15.57–15.44 (5H), 9.09 (4H), 7.90 (4H), 3.46–3.35 (6H), 1.55 (7H), –2.04 (2H) ppm; ^{19}F NMR (376 MHz, toluene-d_8, 0 °C) δ = –9.62, –51.14, –63.42, –73.21 ppm. Anal. Calcd for **4b**: C, 39.65; H, 3.06; N, 2.50. Found: C, 38.89; H, 3.06; N, 2.28. Other attempts at elemental analysis produced similar results. Orange prisms of **4b** suitable for X-ray crystallography were obtained from saturated Et$_2$O/toluene solutions at –25 °C. **4b** crystallizes in the triclinic space group P–1, a = 10.7331(6) Å, b = 10.8919(7) Å, c = 25.2888(16) Å, α= 78.597(3)°, β= 78.146(3)°, γ= 85.050(3)°, Z = 2, GOF on F^2 = 1.058, R indices (all data) R1 = 0.0654, wR2 = 0.1385.

Preparation of Metallacyclobutadiene (**4c**) A 25 mL vial was charged with [TolC≡Mo(OCMe(CF$_3$)$_2$)$_3$(DME)] (**1**) (59.2 mg, 0.071 mmol) in benzene (6 mL). A solution of 1-(phenylethynyl)pyrrolidin-2-one (**2c**) (26.3 mg, 0.142 mmol) in benzene (2 mL) was added. After 1 h, the reaction mixture was concentrated in vacuum. The crude mixture was triturated with pentane and **4c** (54.5 mg, 83 %) was collected as an orange solid. ^{1}H NMR (500 MHz, C$_6$D$_6$, 22 °C) δ = 7.27 (d, J = 8.0 Hz, 2H), 7.21–7.18 (m, 3H), 3.03 (t, J = 8.0 Hz, 4H), 2.93 (t, J = 7.0 Hz, 4H), 2.23 (s, 3H), 1.43 (s, 6H), 1.37 (quint, J = 7.5 Hz, 4H) ppm; ^{19}F NMR (564 MHz, C$_6$D$_6$, 22 °C) δ = –76.65 (s, 6F), –76.78 (s, 3F) ppm; {^{1}H} ^{13}C NMR (151 MHz, C$_6$D$_6$, 22 °C) δ = 238.1, 182.6, 133.5, 129.1, 128.8, 126.6, 126.5, 126.2, 124.6, 124.3, 122.7, 84.9 (m, J_{CF} = 28 Hz), 83.7 (m, J_{CF} = 29 Hz), 46.5, 25.6, 24.2, 17.2, 17.1 ppm; Anal. Calcd for **4c**: C, 37.84; H, 2.85; N, 3.04. Found: C, 37.45; H, 2.78; N, 2.84. Orange plates of **4c** suitable for X-ray crystallography were obtained from saturated Et$_2$O solutions at –25 °C. **4c** crystallizes in the triclinic space group P–1, a = 10.0185(3) Å, b = 10.8539(3) Å, c = 17.1855(5) Å, α= 77.653(2)°, β= 80.752(2)°, γ= 84.727(2)°, Z = 2, GOF on F^2 = 1.067, R indices (all data) R1 = 0.0462, wR2 = 0.0876.

General procedure for ROAMP and termination reaction. A 25 mL vial was charged under Ar with **1** (2.08 mg, 2.5 μmol) in benzene (0.22 mL). **7** (0.025 mmol) in benzene (0.4 mL) was added, and the mixture was stirred for 1 h at 24 °C. Compound **2a-e** (5 μmol) in benzene was added, and the reaction mixture was stirred for 1 h and diluted with MeOH (5 mL). The solid precipitate was isolated by filtration (0.2 μm nylon membrane) and washed with MeOH (10 mL) and hexanes (10 mL) to yield *poly*-**7a-e** as yellow solids (>80%).

*Preparation of poly-**7e**$_{15}$-block-εCL$_{75}$.* A 4 mL vial with septum cap was charged with *poly*-**7e**-OH (9 mg, 1.4 μmol), AlMe(ONO) (1.4 mg, 2.8 μmol) in dry CH$_2$Cl$_2$ (1.5 mL). The mixture was heated at 60 °C for 0.5 h. εCL (18.7 mg, 0.164 mmol) in dry CH$_2$Cl$_2$ (0.2 mL) was added and the reaction mixture heated at 60 °C for 5.5 h. The reaction mixture was diluted with MeOH (15 mL), filtered (0.2 μm nylon membrane), and washed with MeOH to yield crude polymer. The crude polymer was suspended in THF (5mg/mL) and filtered (0.2 μm nylon membrane) to remove residual poly-**7e**-OH yielding *poly-**7e**$_{15}$-block-εCL$_{75}$* (11.1 mg, 66 %) as a colorless solid. ^{1}H NMR (600 MHz, CDCl$_3$, 22 °C) δ = 7.40 (d, J = 8.4 Hz, 30H), 6.70–6.63 (m, 60H), 4.06 (t, J = 6.6 Hz, 93H), 3.67 (t, J = 6.3 Hz, 60H), 3.18 (s, 65H), 2.31 (t, J = 7.5 Hz, 95H), 1.68–1.61 (m, 258H), 1.40–1.25 (m, 342H), 0.91–0.86 (m, 116H) ppm; {^{1}H} ^{13}C NMR (151 MHz, CDCl$_3$, 22 °C) δ = 173.7, 159.2, 145.2, 133.4, 131.6, 131.4, 129.2, 115.3, 114.6, 113.0, 90.5, 67.9, 64.3, 62.8, 36.6, 34.4, 34.3, 32.5, 31.8, 29.4, 28.5, 25.9, 25.7, 24.8, 24.7, 22.7, 14.2 ppm.

ASSOCIATED CONTENT

Supporting Information

The Supporting Information is available free of charge on the ACS Publications website.

GGMS traces (Figure S1-S2)
Computational details (Table S1-S2, Figure S3-S4);
MALDI mass and SEC traces (Figure S5-S18);
DSC traces of polymers (Figure S19)
methods and instrumentation;
synthetic procedures for **2a**, **2d**, and **2e**;
X-ray crystallographic data (Table S3-S12);
NMR spectra (Figure S20-S43)
X-ray data for **4b** (CIF)
X-ray data for **4c** (CIF)

AUTHOR INFORMATION

Corresponding Author

* ffischer@berkeley.edu

Author Contributions

All authors approved the final version of the manuscript.

ACKNOWLEDGMENT

Research supported by the National Science Foundation under contract number CHE-1455289, Berkeley Molecular Graphics and Computation Facility is supported in part by NSF grant CHE-0840505, Berkeley NMR Facility is supported in part by NIH grant SRR023679A, and X-Ray Facility is supported in part by NIH Shared Instrumentation Grant S10-RR027172. The authors acknowledge Dr. Hasan Celik for support with NMR acquisition and Dr. Micah Ziegler and Dr. Antonio DiPasquale for assistance with X-ray analysis, and Dr. Rita Nichiporuk for assistance with mass spectrometry.

REFERENCES

(1) Schrock, R. R. *Acc. Chem. Res.* **1990**, *23* (5), 158–165.
(2) Hilf, S.; Kilbinger, A. F. M. *Nat. Chem.* **2009**, *1* (7), 537–546.
(3) Nomura, K.; Abdellatif, M. M. *Polymer (Guildf).* **2010**, *51* (9), 1861–1881.
(4) Schrock, R. R.; Feldman, J.; Cannizzo, L. F.; Grubbs, R. H. *Macromolecules* **1987**, *20* (5), 1169–1172.
(5) Bazan, G. C.; Khosravi, E.; Schrock, R. R.; Feast, W. J.; Gibson, V. C.; O'Regan, M. B.; Thomas, J. K.; Davis, W. M. *J. Am. Chem. Soc.* **1990**, *112* (23), 8378–8387.
(6) Nomura, K.; Takahashi, S.; Imanishi, Y. *Macromolecules* **2001**, *34* (14), 4712–4723.
(7) Wu, Z.; Nguyen, S. T.; Grubbs, R. H.; Ziller, J. W. *J. Am. Chem. Soc.* **1995**, *117* (20), 5503–5511.
(8) Chen, B.; Metera, K.; Sleiman, H. F. *Macromolecules* **2005**, *38* (4), 1084–1090.
(9) Owen, R. M.; Gestwicki, J. E.; Young, T.; Kiessling, L. L. *Org. Lett.* **2002**, *4* (14), 2293–2296.
(10) Gordon, E. J.; Gestwicki, J. E.; Strong, L. E.; Kiessling, L. L. *Chem. Biol.* **2000**, *7* (1), 9–16.
(11) Murphys, J. J.; Furusho, H.; Paton, R. M.; Nomura, K. *Chem. - A Eur. J.* **2007**, *13* (32), 8985–8997.
(12) Gu, W.; Huh, J.; Hong, S. W.; Sveinbjornsson, B. R.; Park, C.; Grubbs, R. H.; Russell, T. P. *ACS Nano* **2013**, *7* (3), 2551–2558.
(13) Kawamoto, K.; Zhong, M.; Gadelrab, K. R.; Cheng, L.-C.; Ross, C. A.; Alexander-Katz, A.; Johnson, J. A. *J. Am. Chem. Soc.* **2016**, *138* (36), 11501–11504.
(14) Xia, Y.; Olsen, B. D.; Kornfield, J. A.; Grubbs, R. H. *J. Am. Chem. Soc.* **2009**, *131* (51), 18525–18532.

(15) Gestwicki, J. E.; Cairo, C. W.; Mann, D. A.; Owen, R. M.; Kiessling, L. L. *Anal Biochem* **2002**, *305* (2), 149–155.
(16) Albagli, D.; Bazan, G. C.; Schrock, R. R.; Wrighton, M. S. *J. Am. Chem. Soc.* **1993**, *115* (16), 7328–7334.
(17) Àrias, Ò.; Brandhorst, K.; Baabe, D.; Freytag, M.; Jones, P. G.; Tamm, M. *Dalt. Trans.* **2017**, *46* (14), 4737–4748.
(18) DeKorver, K. a; Li, H.; Lohse, A. G.; Hayashi, R.; Lu, Z.; Zhang, Y.; Hsung, R. P. *Chem. Rev.* **2010**, *110*, 5064–5106.
(19) von Kugelgen, S.; Sifri, R.; Bellone, D.; Fischer, F. R. *J. Am. Chem. Soc.* **2017**, *139* (22), 7577–7585.
(20) Pilyugina, T. S.; Schrock, R. R.; Hock, A. S.; Müller, P. *Organometallics* **2005**, *24* (8), 1929–1937.
(21) Pyykkö, P.; Atsumi, M. *Chem. - A Eur. J.* **2009**, *15* (46), 12770–12779.
(22) O'Reilly, M. E.; Ghiviriga, I.; Abboud, K. A.; Veige, A. S. *Dalt. Trans.* **2013**, *42* (10), 3326–3336.
(23) Beer, S.; Hrib, C. G.; Jones, P. G.; Brandhorst, K.; Grunenberg, J.; Tamm, M. *Angew. Chemie Int. Ed.* **2007**, *46* (46), 8890–8894.
(24) Pedersen, S. F.; Schrock, R. R.; Churchill, M. R.; Wasserman, H. J. *J. Am. Chem. Soc.* **1982**, *104* (24), 6808–6809.
(25) Churchill, M. R.; Ziller, J. W.; Freudenberger, J. H.; Schrock, R. R. *Organometallics* **1984**, *3* (10), 1554–1562.
(26) Freudenberger, J. H.; Schrock, R. R.; Churchill, M. R.; Rheingold, A. L.; Ziller, J. W. *Organometallics* **1984**, *3* (10), 1563–1573.
(27) Churchill, M. R.; Ziller, J. W. *J. Organomet. Chem.* **1985**, *286* (1), 27–36.
(28) Townsend, E. M.; Kilyanek, S. M.; Schrock, R. R.; Müller, P.; Smith, S. J.; Hoveyda, A. H. *Organometallics* **2013**, *32* (16), 4612–4617.
(29) Von Kugelgen, S.; Bellone, D. E.; Cloke, R. R.; Perkins, W. S.; Fischer, F. R. *J. Am. Chem. Soc.* **2016**, *138* (19), 6234–6239.
(30) Chen, C. T.; Huang, C. A.; Huang, B. H. *Macromolecules* **2004**, *37* (21), 7968–7973.
(31) Bellone, D. E.; Bours, J.; Menke, E. H.; Fischer, F. R. *J. Am. Chem. Soc.* **2015**, *137* (2), 850–856.
(32) Hamada, T.; Ye, X.; Stahl, S. S. *J. Am. Chem. Soc.* **2008**, *130* (3), 833–835.
(33) Theunissen, C.; Lecomte, M.; Jouvin, K.; Laouiti, A.; Guissart, C.; Heimburger, J.; Loire, E.; Evano, G. *Synthesis (Stuttg).* **2014**, *46* (9), 1157–1166.

Insert Table of Contents artwork here